



## RESEARCH PAPER

# Difference in root $K^+$ retention ability and reduced sensitivity of $K^+$ -permeable channels to reactive oxygen species confer differential salt tolerance in three *Brassica* species

Koushik Chakraborty<sup>1,2</sup>, Jayakumar Bose<sup>2,\*</sup>, Lana Shabala<sup>2</sup> and Sergey Shabala<sup>2,†</sup>

<sup>1</sup> Department of Plant Physiology, ICAR-Directorate of Groundnut Research, Junagadh, Gujarat-362 001, India

<sup>2</sup> School of Land and Food and Tasmanian Institute for Agriculture, University of Tasmania, Hobart, Private Bag 94, Tas 7001, Australia

\* Present address: School of Agriculture, Food and Wine, University of Adelaide, PMB1, Glen Osmond, SA 5064, Australia.

† Correspondence: [Sergey.Shabala@utas.edu.au](mailto:Sergey.Shabala@utas.edu.au)

Received 13 April 2016; Accepted 25 May 2016

Editor: Christine Raines, University of Essex

## Abstract

***Brassica* species are known to possess significant inter and intraspecies variability in salinity stress tolerance, but the cell-specific mechanisms conferring this difference remain elusive. In this work, the role and relative contribution of several key plasma membrane transporters to salinity stress tolerance were evaluated in three *Brassica* species (*B. napus*, *B. juncea*, and *B. oleracea*) using a range of electrophysiological assays. Initial root growth assay and viability staining revealed that *B. napus* was most tolerant amongst the three species, followed by *B. juncea* and *B. oleracea*. At the mechanistic level, this difference was conferred by at least three complementary physiological mechanisms: (i) higher  $Na^+$  extrusion ability from roots resulting from increased expression and activity of plasma membrane SOS1-like  $Na^+/H^+$  exchangers; (ii) better root  $K^+$  retention ability resulting from stress-inducible activation of  $H^+$ -ATPase and ability to maintain more negative membrane potential under saline conditions; and (iii) reduced sensitivity of *B. napus* root  $K^+$ -permeable channels to reactive oxygen species (ROS). The last two mechanisms played the dominant role and conferred most of the differential salt sensitivity between species. *Brassica napus* plants were also more efficient in preventing the stress-induced increase in *GORK* transcript levels and up-regulation of expression of *AKT1*, *HAK5*, and *HKT1* transporter genes. Taken together, our data provide the mechanistic explanation for differential salt stress sensitivity amongst these species and shed light on transcriptional and post-translational regulation of key ion transport systems involved in the maintenance of the root plasma membrane potential and cytosolic K/Na ratio as a key attribute for salt tolerance in *Brassica* species.**

**Key words:**  $H^+$ -ATPase, ion homeostasis, membrane potential, potassium retention, ROS detoxification, sodium exclusion, tissue tolerance.

## Introduction

In today's context of global climate change, salinization of arable land is a major threat to the agricultural production system. Although improving salt tolerance in major cultivated crops is of paramount importance to global food security in the 21st

century, the process is significantly handicapped by the physiological and genetic complexity of the salinity tolerance trait and, as such, requires understanding of the orchestrated regulation of major subtraits at the tissue-specific level (Zhu, 2001).

Oilseeds and vegetables are two very important components of human food and are dietary necessities. The family *Brassicaceae* includes a number of cultivated crop species that have a considerable degree of variation in their salt tolerance (Purty *et al.*, 2008; Kumar *et al.*, 2009; Chakraborty *et al.*, 2016a). A considerable inter- and intraspecific variation in the overall growth, electrolyte leakage, proline accumulation, and maintenance of the  $K^+/Na^+$  ratio was observed for different *Brassica* species (Ashraf and McNeilly, 2004; Purty *et al.*, 2008; Chakraborty *et al.*, 2012). At the whole-plant level, the mechanism of salt tolerance varied considerably among three *Brassica* species (*B. napus*, *B. juncea*, and *B. oleracea*) tested with 150 mM NaCl stress (Chakraborty *et al.*, 2016b). It was shown that the overall superior salinity stress tolerance in *B. napus* was achieved by the higher osmo-tolerance matched by the moderate tissue tolerance and superior  $K^+$  retention ability in the leaf mesophyll. At the same time, while showing relatively modest overall tolerance, *B. oleracea* was far more superior in terms of shoot tissue tolerance. However, to the best of our knowledge, no specific details on the molecular/cellular mechanisms conferring this intra- and inter-specific variability in salinity tolerance are available in the literature, and no significant quantitative trait locus (QTL) related to salinity tolerance has been identified in *Brassica* to date (Nayidu *et al.*, 2013).

For the majority of glycophytes, salinity tolerance is achieved through more than one strategy operating either simultaneously or in isolation, depending upon the duration and intensity of the stress (Munns, 2002). Such strategies include improved osmotic adjustment, exclusion of  $Na^+$  from uptake, intracellular  $Na^+$  sequestration,  $K^+$  retention in the cytosol, control of xylem ion loading, and oxidative stress tolerance (Ashraf *et al.*, 2008; Adem *et al.*, 2014; Bose *et al.*, 2014a). Which of these make the greatest contribution to salinity stress tolerance in *Brassica*?

Many glycophytes including cultivated crop species employ  $Na^+$  exclusion and/or partitioning strategies to achieve salt tolerance. Induced expression of the plasma membrane  $Na^+/H^+$  antiporter (encoded by the *SOS1* gene in Arabidopsis) results in improved salt tolerance in several species (Zhu, 2001). In contrast, the Arabidopsis *salt overly sensitive1* (*sos1*) mutant, not having the capacity to exclude  $Na^+$  from its uptake, was found to accumulate 5-fold more  $Na^+$  in the shoot tissue and showed a highly sensitive phenotype (Nublat *et al.*, 2001). Unlike *SOS1* which pumps cytosolic  $Na^+$  into the apoplastic space, the tonoplast-based *NHX1*  $Na^+/H^+$  antiporter removes cytotoxic  $Na^+$  by pumping it into the vacuole for sequestration (Fan *et al.*, 2015). At the same time, no significant difference in unidirectional (channel-mediated)  $Na^+$  uptake was reported between genotypes contrasting in salinity stress tolerance in various crop species [e.g. wheat (Davenport *et al.*, 2005) and barley (Chen *et al.*, 2007)]. Is this also the case for *Brassica*?

Another important aspect of achieving tissue tolerance is through maintenance of  $K^+$  homeostasis (Anschutz *et al.*, 2014; Shabala *et al.*, 2016a). By screening nearly 70 barley varieties contrasting in salinity stress tolerance, Chen *et al.*

(2007) showed that >60% of genetic variability in salinity stress tolerance in barley was related to the roots' ability to retain  $K^+$  in the mature root zone upon acute NaCl treatment. Similar reports were later published for wheat (Cuin *et al.*, 2008), lucerne (Smethurst *et al.*, 2008), and poplar (Sun *et al.*, 2009), and strong evidence for the inheritance of this trait was provided (Chen *et al.*, 2008; Cuin *et al.*, 2011). At the same time, NaCl-induced  $K^+$  efflux from wheat roots was shown to be an order of magnitude smaller compared with barley, for the same experimental conditions (for comparison, see Chen *et al.*, 2007; Cuin *et al.*, 2009). Does  $K^+$  retention in roots play a major role in salinity stress tolerance in *Brassica*? If the answer is yes, how is this  $K^+$  retention achieved? Does this occur at the transcriptional or post-translational level? Several pathways were reported to mediate NaCl-induced  $K^+$  efflux from plant tissues. These are highly tissue specific and include (Wu *et al.*, 2015; Shabala *et al.*, 2016a): (i) depolarization-activated outward-rectifying  $K^+$ -selective channels; (ii) weakly voltage-dependent non-selective cation channels (NSCCs); and (iii) reactive oxygen species (ROS)-activated  $K^+$ -permeable channels. Which of these pathways (if any) operates in *Brassica* roots?

Previous reports also suggested that cytosolic  $Ca^{2+}$  signalling is an essential component of plant adaptation to saline conditions (Dodd *et al.*, 2010). At least several concurrent signalling loops have to be considered. One of them is related to the salt overly sensitive (SOS) pathway. The activity of *SOS1* is regulated by the CBL–CIPK complex that is achieved by phosphorylating its C-terminus (Quintero *et al.*, 2011). To enable this activation, a salt stress-induced  $Ca^{2+}$  signal is first detected by *SOS3* (CBL4), a myristoylated calcium-binding protein; *SOS3* is then activated by recruiting *SOS2* (CIPK24), a serine/threonine protein kinase (reviewed in Shabala *et al.*, 2015). Elevated apoplastic  $Ca^{2+}$  levels are also essential to NSCC-mediated  $Na^+$  uptake (Demidchik and Tester, 2002) and prevent  $K^+$  leakage from the cell (Shabala *et al.*, 2006). Finally, salinity stress results in a substantial build-up of the cytotoxic hydroxyl radical and induces  $K^+$  efflux and  $Ca^{2+}$  influx in both root and shoot tissues (Demidchik *et al.*, 2003, 2010), with NADPH oxidase being one of the major sources of such ROS production and accumulation in the apoplast (Bose *et al.*, 2014b; Demidchik, 2015; Shabala *et al.*, 2015). Also, both constitutive and ROS-induced ion fluxes could vary significantly between different parts of the root (i.e. the mature and elongation zone) (Demidchik *et al.*, 2007). In this context, it was shown that the  $Ca^{2+}$  transport protein Annexin 1 in *Arabidopsis thaliana* (AtANN1) mediates root responses to extracellular  $H_2O_2$  (Laohavisit *et al.*, 2012), and so are cyclic nucleotide-gated  $Ca^{2+}$ -permeable channels (Ordóñez *et al.*, 2014). What role do  $Ca^{2+}$  transport systems play in *Brassica* root responses to salinity?

The present study attempted to address the above questions by conducting a detailed electrophysiological investigation of mechanisms underlying interspecific variability in salinity stress tolerance in *Brassica*, at the tissue level. The

non-invasive micro-electrode ion flux estimation (MIFE) technique was employed to study the kinetics of stress-induced net fluxes of  $\text{Na}^+$ ,  $\text{K}^+$ ,  $\text{Ca}^{2+}$ , and  $\text{H}^+$  from various root zones and then link these changes with changes in the transcriptional profile of several key candidate genes. The molecular identity of the transporters involved was further confirmed in a series of pharmacological experiments.

## Materials and methods

### *Plant material and experimental condition*

The *Brassica* seeds of three different species, namely *B. napus*, *B. juncea*, and *B. oleracea*, were obtained from commercial suppliers (Zepson Seeds, Richmond and Hollander Imports, Hobart, Australia). Seeds were surface sterilized with 1% (v/v) HClO for 10 min, thoroughly rinsed with distilled water, and then grown using the paper roll method (Pandolfi *et al.*, 2010) in non-buffered basic salt medium (BSM) solution (0.5 mM KCl+0.2 mM NaCl+0.1 mM  $\text{CaCl}_2$ , pH 5.7) in the dark for 4–5 d at room temperature ( $24 \pm 1^\circ\text{C}$ ). Plants were used for electrophysiological measurements when their root length was between 50 mm and 70 mm.

For long-term salinity treatment experiments [root growth assay, viability staining, membrane potential (MP), steady-state  $\text{Na}^+$  flux measurement, and gene expression studies], the seeds of all three *Brassica* species were surfaced sterilized and placed in paper rolls, and allowed to germinate and grow for 3 d in dark as described above. Then the uniformly grown seedlings were transferred to a 1.5 litre plastic container of aerated BSM added with the appropriate strength of NaCl as per the treatment requirement. The seedlings were suspended on a plastic grid so that their roots were completely immersed in the BSM. Plants were then grown under 16/8 h light/dark cycle at  $24^\circ\text{C}$  air temperature with an irradiance of  $150 \mu\text{mol m}^{-2} \text{s}^{-1}$  for another 2–4 d.

### *Root growth assay*

Root length was measured from control and 150 mM NaCl-treated plants, which were subjected to at least 48 h of salt treatment. The reduction in the root length of salt-treated seedlings was expressed as a percentage of the control by comparing them with plants of the same age grown in BSM without salt.

### *Viability staining*

For viability staining, the *Brassica* seeds were grown in BSM without (control) and with NaCl added (treatment) as described above and the roots were collected after 2 d of 150 mM NaCl treatment. The viability of the *Brassica* roots was assessed by using the fluorescein diacetate (FDA)–propidium iodide (PI) double staining method as described in Koyama *et al.* (1995). FDA (Cat. No. F7378; Sigma, St. Louis, MO, USA) is a non-polar ester permeable through the intact plasma membrane, and shows green colour under a fluorescent microscope in viable cells after hydrolysis by the internal esterases, while PI (Cat. No. P4864; Sigma-Aldrich) is impermeable to the intact plasma membrane and enters only cells with a damaged plasma membrane with large pores (i.e. dead or dying cells), which is indicated by red colour under a fluorescent light upon PI–nuclear DNA conjugate formation.

Control and 150 mM NaCl-treated seedlings were stained in the darkness with freshly prepared FDA solution ( $5 \mu\text{g ml}^{-1}$ ) for 3 min, followed by PI solution ( $3 \mu\text{g ml}^{-1}$ ) for 10 min. The double-stained roots were observed under a fluorescence microscope (Leica MZ12; Leica Microsystems, Wetzlar, Germany) illuminated by an ultra-high-pressure mercury lamp (Leica HBO Hg 100 W; Leica Microsystems) and fitted with a Leica I3-wavelength filter cube (Leica Microsystems). The excitation and emission wavelengths were 488/505–530 nm and 543/585 nm for FDA and PI, respectively. Photographs were taken with a Leica (DFC295; Leica Microsystems) camera fitted on the

microscope using image acquisition and processing software LAS V3.8 (Leica Microsystems). During image acquisition, all the automatic exposure features of the LAS V3.8 were disabled, and exposure time (0.62 s), gain (2.3 $\times$ ), saturation (0.35), and gamma (2.37) were set to constant values for all the measurements. To determine the extent of cell death, the red and green channels of the fluorescent images were separated and the fluorescent intensity of the respective images was quantified using Fiji (ImageJ) software.

### *Ion flux measurements*

Net fluxes of  $\text{H}^+$ ,  $\text{K}^+$ ,  $\text{Ca}^{2+}$ , and  $\text{Na}^+$  were measured by a non-invasive ion flux measurement technique using vibrating ion-selective microelectrodes (the MIFE technique; University of Tasmania) as described previously (Cuin *et al.*, 2011; Wu *et al.*, 2015). Briefly, microelectrodes were prepared from borosilicate glass capillaries by pulling capillaries followed by drying and silanization with tributylchlorosilane. The electrode tips were broken to achieve external tip diameters of 2–3  $\mu\text{m}$  before they were backfilled with the corresponding back-filling solutions, followed by front-filling with appropriate ion-selective cocktails (see Supplementary Table S1 at JXB online).

Electrodes were mounted on a 3D-micromanipulator (MMT-5, Narishige) and calibrated in an appropriate set of standards encompassing measured ranges of particular ions using a three-point calibration. For MIFE measurements, the plant sample with intact roots (already adapted to BSM for 40 min) was immobilized in a measuring chamber, mounted on a microscope stage, and electrode tips positioned 40  $\mu\text{m}$  away from the root surface. Net fluxes were measured from the elongation (800–1000  $\mu\text{m}$  from the root tip) and mature (20 mm from the root tip) root zones. The electrochemical potential difference between the two positions was recorded for each electrode by the MIFE CHART software (Shabala *et al.*, 1997) and converted to ion concentration difference using the calibrated Nernst slope of the electrode. Net ion fluxes were calculated using the MIFEFLUX software for cylindrical diffusion geometry (Newman, 2001). All treatments [either 150 mM NaCl for salinity stress; or 0.3 mM  $\text{CuCl}_2$ +1 mM Na-ascorbate (referred to as Cu/A) for oxidative stress] were applied after recording steady fluxes of the respective ions for at least 5 min. For the steady-state  $\text{Na}^+$  flux measurements, both the control and roots treated with 150 mM NaCl for 48 h were immobilized as described above and net fluxes were recorded for at least 5 min from the mature and elongation zones.

### *Pharmacology*

In pharmacological experiments, plant roots were pre-treated for 30–60 min prior to application of NaCl or Cu/A stresses with one of the following: 1 mM sodium orthovanadate (vanadate; a potent blocker of the  $\text{H}^+$ -ATPase pump; Sigma, Cat. S6508); 1 mM amiloride (a potent blocker of  $\text{Na}^+/\text{H}^+$  antiport; Sigma Cat. A4562); or 1  $\mu\text{M}$  Eosin Yellow (EY; a known blocker of the  $\text{Ca}^{2+}$ -ATPase pump; Sigma Cat. 119830).

### *Membrane potential measurement*

Both control and salt-treated seedlings were immobilized in a measuring chamber as described earlier (Bose *et al.*, 2014a) and were kept for pre-conditioning in BSM (with/without NaCl) for 50–60 min. A conventional microelectrode (GC 150F-10, Harvard Apparatus Ltd, Kent, UK) with a tip diameter of  $\sim 0.5 \mu\text{m}$  was filled with 0.5 M KCl and connected to a MIFE electrometer (Shabala *et al.*, 1997) via an Ag–AgCl half-cell. The mounted electrode was then impaled in the external cortex cells of intact roots using a manually operated hydraulic micromanipulator (MHW-4-1; Narishige, Tokyo, Japan). The steady-state MP measurements were conducted from at least six individual roots (from both the mature and elongation zones as described above) with no more than four impalements per root



undertaken. Each measurement was averaged for at least a 30 s interval (Bose *et al.*, 2014a).

#### Gene expression study

For gene expression studies, *Brassica* seedlings grown as described earlier were subjected to 150mM NaCl stress for a period for 1 h and 48 h in order to simulate the short- and long-term salt stress condition, which finally correlated with ion flux measurement and other root growth studies. Total RNAs from root tissues of control and salt-treated plants were isolated using the RNASure Plant Kit (Genetix Brand, Cat NP-84905) according to the manufacturer's protocol, with minor modifications. Briefly, root tissues (~100 mg) were homogenized in liquid nitrogen to a fine powder and suspended in lysis buffer, before they were subjected to on-column DNase digestion to eliminate any genomic DNA contamination. Finally, the RNA pellet was re-suspended in 20  $\mu$ l of RNase-free water and stored at -20 °C for further use. The integrity of the RNA was confirmed in the gel, and the absorbance of the isolated RNA was recorded using a Nanodrop Spectrophotometer (ND 1000). Approximately 2  $\mu$ g of total RNA was used for cDNA synthesis using a First strand cDNA synthesis kit (Thermo Scientific), and the synthesized cDNA was confirmed by PCR using all cDNA samples (~100 ng) as template with an 18S rRNA primer. To test gene-specific primers (see Supplementary Table S2 for sequence details), the above experiment was carried out for each set of primers and a single amplicon PCR product was confirmed in agarose gel.

Changes in expression of the above genes (transcript levels) were studied by real-time quantitative PCR (StepOnePlus™ Real-Time PCR System from Applied Biosystems using a QuantiFast SYBR Green PCR kit, Qiagen, USA). The reaction mixture included ~100 ng of cDNA, 0.16  $\mu$ M of primers, and 12.5  $\mu$ l of QuantiFast SYBR Green PCR mix. The reaction volume was maintained at 20  $\mu$ l by sterile nuclease-free water. Reactions were run under the following conditions: 95 °C for 5 min for one cycle; 95 °C for 10 s and 60 °C for 30 s for 40 cycles. At the end of the PCR cycles, the products were put through a melt curve analysis to determine the specificity of amplification. The fold changes in transcript in salt-treated roots were compared with those of control plants in terms of fold change, analysed by the comparative  $2^{-\Delta\Delta Ct}$  method (Schmittgen and Livak, 2008). The *Br-18s rRNA* gene was used as the internal control to normalize the PCRs (Sarkar *et al.*, 2014).

## Results

*Differential salt sensitivity was observed in three Brassica species under both short- and long-term salinity stress*

The three *Brassica* species (*B. napus*, *B. juncea*, and *B. oleracea*) do vary significantly in terms of tolerance to salinity stress when studied in long-term experiments under glasshouse or field conditions (Ashraf and McNeilly, 2004; Chakraborty *et al.*, 2016b). This differential salt sensitivity is phenotypically detected even under a much shorter duration of stress. Significant differences in the root growth rate were found in 5-day-old seedlings grown under control and saline (150mM NaCl) conditions (Fig. 1). The visible difference in the root growth (Fig. 1A) of salt-treated plants suggested the order of salt tolerance as *B. napus* > *B. juncea* > *B. oleracea*, at the seedling stage. Under control conditions, the root growth varied between 8 cm and 10 cm in 5-day-old seedlings of the three *Brassica* species tested. Treatment with 150 mM NaCl restricted root growth to a mere ~30% and ~50% in the case of *B. oleracea* and *B. juncea*, respectively, while there was nearly 75% retention of root length in *B. napus* compared with control plants (Figs 1B, C).

The three *Brassica* species showed distinctive variability in the tissue-specific sensitivity to salt stress, as revealed by viability staining experiments (Fig. 2A). After 48 h of 150 mM NaCl treatment, the root tip of *B. napus* (most tolerant) was almost as healthy as non-treated root, while both *B. juncea* (>25% mortality) and *B. oleracea* (>50% mortality) showed a considerably higher level of mortality around the root tip (Fig. 2B, C). Unlike *B. napus* and *B. juncea*, *B. oleracea*, showed symptoms of dying from the root tip spreading towards the mature zone upon long-term salt exposure. Similar to the elongation zone, the mature zone of all the three species showed loss of viability to different extents, with *B. napus* being the least damaged (~10%), while *B. juncea*

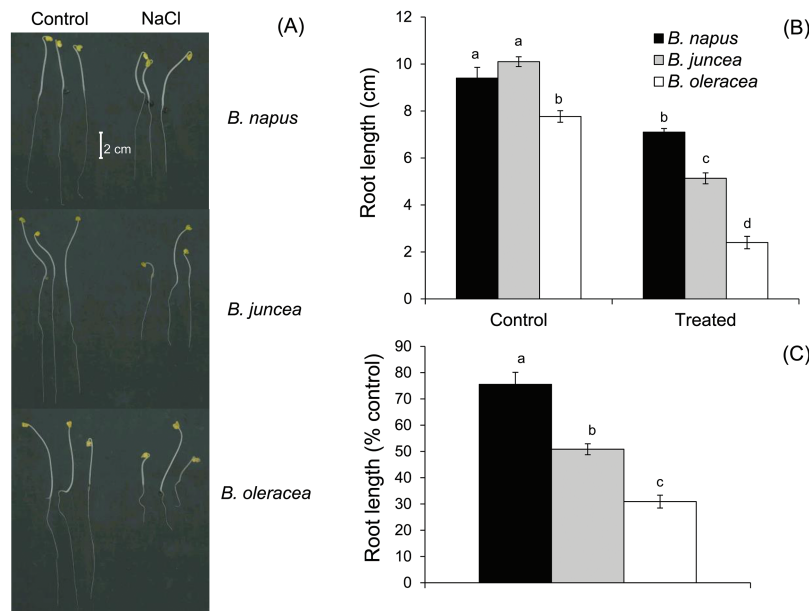


**Fig. 1.** Effect of salinity stress on root growth of three *Brassica* species (5-day-old seedling) grown in non-buffered basic salt medium (BSM) solution (0.5 mM KCl+0.2 mM NaCl+0.1 mM CaCl<sub>2</sub>, pH 5.7) and exposed to 150 mM NaCl stress for 72 h. Values are the mean  $\pm$ SE ( $n=5$  individual plants).

(~30%) and *B. oleracea* (~50%) exhibited comparatively much higher loss of viability (Fig. 2B, C).

*Mature and elongation zones behaved differently in terms of Na<sup>+</sup> exclusion and sensitivity towards salt stress*

Addition of 150mM NaCl to the root medium resulted in a massive Na<sup>+</sup> uptake in plant roots (Fig. 3), in both the elongation (Fig. 3A) and mature (Fig. 3B) zones, although with rather different magnitude (~2-fold higher in the root apex). This uptake gradually slowed down, and net Na<sup>+</sup> efflux was measured from *B. napus* roots at ~15 min after onset of 150mM NaCl stress in both zones. In the other two species, however, net Na<sup>+</sup> flux significantly decreased (to nearly zero) but never turned into net efflux (Fig. 3A, B). Also different were the peak magnitudes of net Na<sup>+</sup> uptake immediately after NaCl application. In the mature zone (the major bulk of the root), the most tolerant *B. napus* had a peak value of  $15\,000 \pm 2200 \text{ nmol m}^{-2} \text{ s}^{-1}$ , while it was much higher in *B. juncea* (>2-fold) and *B. oleracea* (>3.5-fold). Also, *B. napus* was able to extrude Na<sup>+</sup> in the mature zone (Fig. 3B), while both *B. juncea* and *B. oleracea* showed net Na<sup>+</sup> uptake of ~3500 nmol m<sup>-2</sup> s<sup>-1</sup> and ~8000 nmol m<sup>-2</sup> s<sup>-1</sup>, respectively, 30 min after the salt treatment. The above findings reported for transient Na<sup>+</sup> fluxes were further confirmed in experiments involving long-term salinity treatments. Root exposure to 150mM NaCl for 48h showed that *B. napus* had 2-fold less steady-state Na<sup>+</sup> uptake in the mature zone compared with the two other *Brassica* species (Fig. 3C) and was the only species that

showed a statistically significant net Na<sup>+</sup> efflux of ~425 nmol m<sup>-2</sup> s<sup>-1</sup> in the elongation zone (Fig. 3C), while the other two species showed only net Na<sup>+</sup> uptake (Fig. 3C).

A series of pharmacological experiments was conducted to reveal the identity of the above strong Na<sup>+</sup> exclusion mechanism in *B. napus*. Pre-treatment of roots with sodium orthovanadate (a known blocker of H<sup>+</sup>-ATPase) and amiloride (an inhibitor of the Na<sup>+</sup>/H<sup>+</sup> plasma membrane exchanger; Cuin *et al.*, 2011) for 1h completely changed the pattern of Na<sup>+</sup> fluxes in *B. napus* roots (Fig. 3D). Both chemicals shifted net Na<sup>+</sup> fluxes towards more positive values by increasing the peak magnitude of net Na<sup>+</sup> uptake by >2.5-fold and ~5-fold for vanadate and amiloride treatment, respectively. Also, no net Na<sup>+</sup> efflux was measured in either treatment at the end of the transient recordings (Fig. 3D). While control plants showed a net Na<sup>+</sup> efflux of  $-3800 \pm 2700 \text{ nmol m}^{-2} \text{ s}^{-1}$  after 30min of NaCl treatment, amiloride-treated roots had a net Na<sup>+</sup> uptake of  $1500 \pm 1250 \text{ nmol m}^{-2} \text{ s}^{-1}$ . These results strongly suggest that the Na<sup>+</sup> exclusion mechanism in *B. napus* is mediated by the plasma membrane-localized Na<sup>+</sup>/H<sup>+</sup> antiporter fuelled by H<sup>+</sup>-ATPase.

*K<sup>+</sup> flux kinetics in mature and elongation zones upon salinity treatment*

The strong efflux of K<sup>+</sup> was observed upon addition of NaCl to the bath medium in both the elongation and mature zones of all the three species, although the pattern differed significantly between the two root zones (Fig. 4A, B). In the elongation zone, the peak K<sup>+</sup> efflux

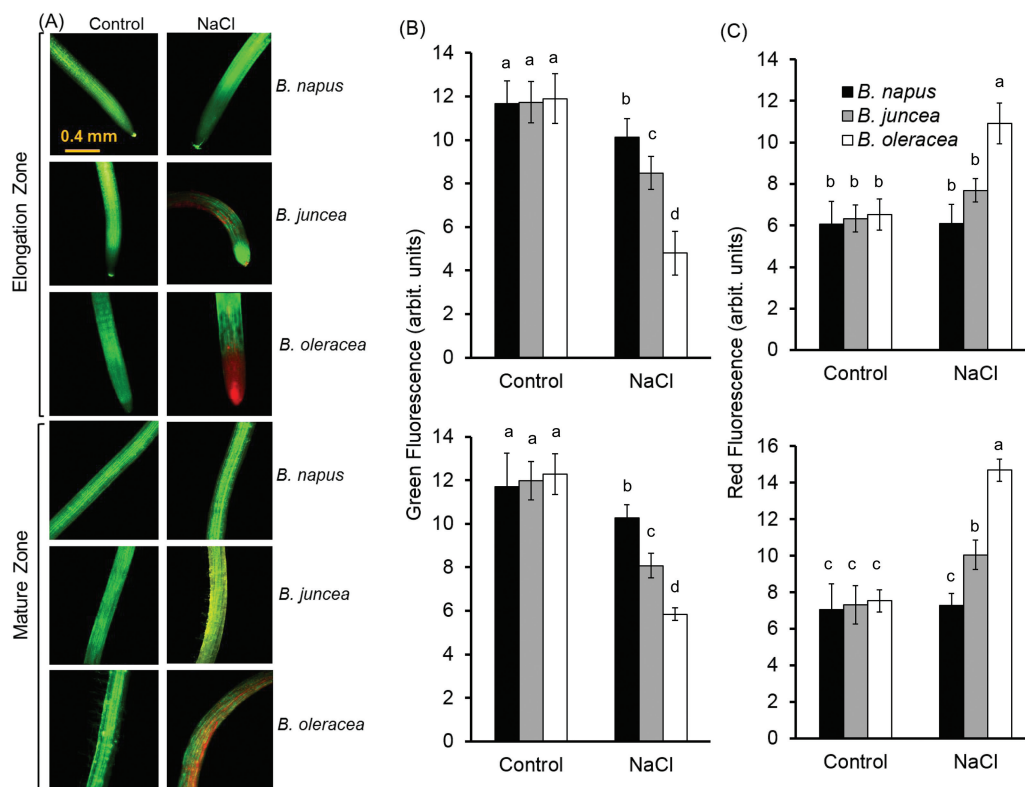


**Fig. 2.** Viability staining of the elongation and mature root zones of three *Brassica* species exposed to 150mM NaCl stress for 48h. (A) One (of five) typical image is shown for each treatment/species. (B, C) Intensity of the green (B) and red (C) fluorescent signal. Values are the mean  $\pm$ SE ( $n=15-20$ ).

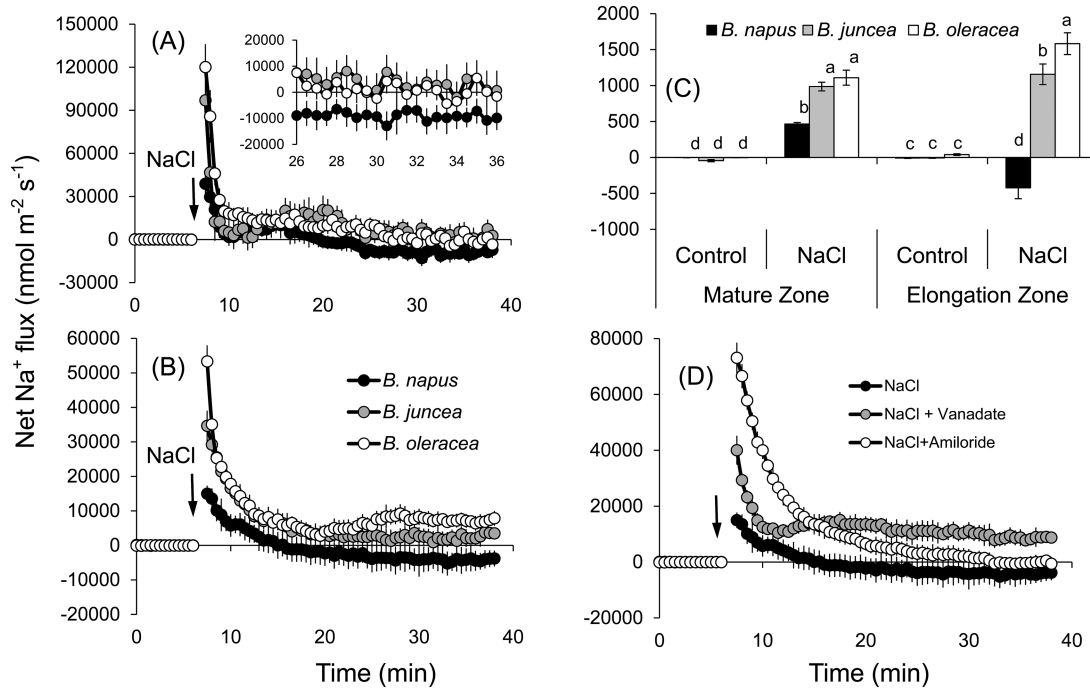


**Fig. 3.** Transient net Na<sup>+</sup> flux kinetics measured in three *Brassica* species from elongation (A) and mature (B) root zones in response to 150mM NaCl stress. The inset in (A) resolves a genotypic difference in the net Na<sup>+</sup> efflux at the end of the transient recording. (C) Steady-state Na<sup>+</sup> efflux from roots (both mature and elongation zones) of three *Brassica* species exposed to 150mM NaCl stress for 48h. (D) Transient net Na<sup>+</sup> flux kinetics in response to 150mM NaCl treatment measured from the mature root zone of *B. napus* pre-treated for 1h in solutions containing a specific metabolic inhibitor or a channel blocker. Values are the mean ±SE (n=6–8). The sign convention for all MIFE measurements is ‘efflux negative’.

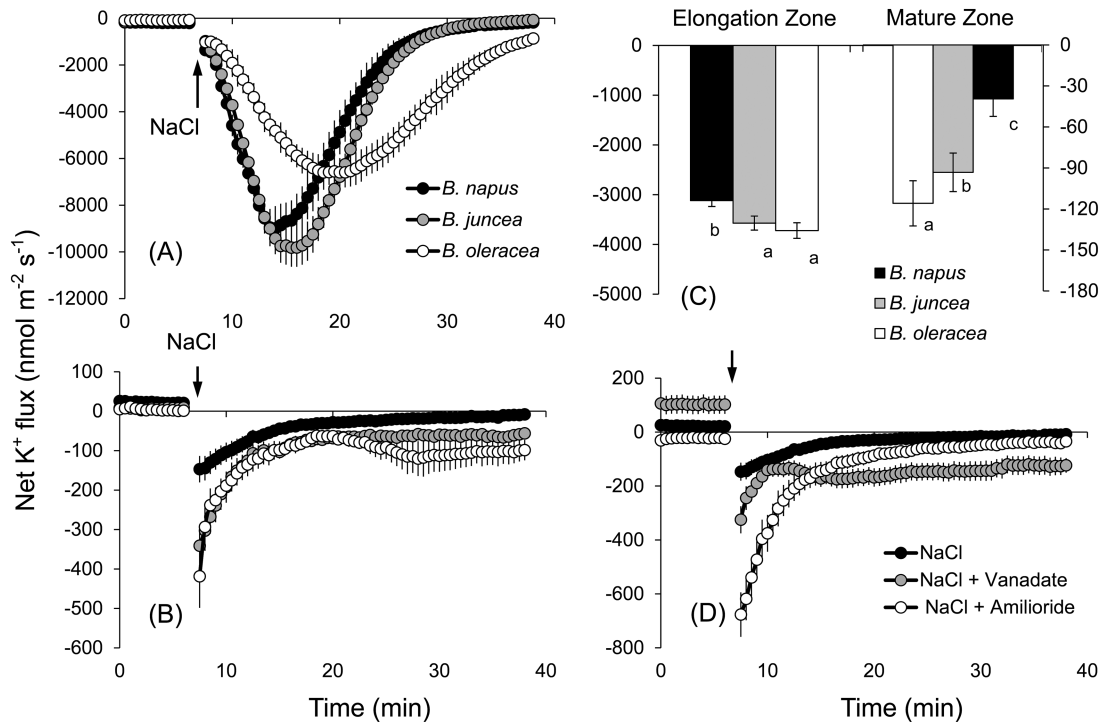


**Fig. 4.** Transient net K<sup>+</sup> flux kinetics measured in three *Brassica* species from the elongation (A) and mature (B) root zones in response to 150mM NaCl stress. (C) Average K<sup>+</sup> flux from roots over the 30min period after Na<sup>+</sup> addition to three *Brassica* species (both mature and elongation zones). (D) Transient net K<sup>+</sup> flux kinetics in response to 150mM NaCl treatment measured from the mature root zone of *B. napus* pre-treated for 1h in solutions containing specific metabolic inhibitors. Values are the mean ±SE (n=6–8).

was highest in *B. juncea* followed by *B. napus* and *B. oleracea*. The salt-induced K<sup>+</sup> leakage was slowly restored to the pre-stress values in *B. napus* and *B. juncea* 25 min after

the stress application, while K<sup>+</sup> efflux in *B. oleracea* persisted throughout the duration of the flux measurements (up to 40 min in Fig. 4A; indicated as negative flux values).

We also observed a delay in the timing of peak  $K^+$  efflux which occurred  $5 \pm 1$  min (*B. napus*),  $7 \pm 0.5$  min (*B. juncea*), and  $14 \pm 2$  min (*B. oleracea*) after application of the stress (Fig. 4A). The overall amount of  $K^+$  leaked over the 30 min interval since the stress (calculated as the area under the curve in the respective graphs) was the smallest in the most tolerant *B. napus* (Fig. 4C, left panel; significant at  $P < 0.05$ ). In the mature zone, the highest  $K^+$  efflux (peak value) was observed immediately after the imposition of a salt stress. This flux was slowly restored to pre-stress values in *B. napus* (Fig. 4B) while it remained highly negative (net  $K^+$  efflux) in the other two varieties (significant at  $P < 0.05$ ). The magnitude of the peak  $K^+$  efflux also varied between the three species, with minimum values observed in *B. napus* followed by *B. juncea* and *B. oleracea*. Similar to the elongation zone, the overall salt-induced  $K^+$  leakage was the highest in the most salt-sensitive species *B. oleracea* and the least leakage was observed in the most salt-tolerant *B. napus* (Fig. 4C, right panel). Pre-treatment of *B. napus* (the most salt tolerant among the varieties tested) with vanadate resulted in a higher peak  $K^+$  efflux and the loss of the ability to restore  $K^+$  values to the pre-stress level (Fig. 4D), suggesting involvement of  $H^+$ -ATPase. Pre-treatment of roots with 1 mM amiloride led to a >4-fold increase in the peak  $K^+$  efflux and remained higher (more negative) than the respective value without the inhibitor 30 min after the treatment ( $-80 \pm 15$   $\text{nmol m}^{-2} \text{s}^{-1}$  and  $0 \pm 8$   $\text{nmol m}^{-2} \text{s}^{-1}$ , respectively). Taken together, the observed results suggest

involvement of the voltage-gated  $K^+$  channels in  $K^+$  retention in *Brassica* roots under salt stress.

*Brassica napus* spends more energy through active  $H^+$  pumping for maintaining the membrane potential under salinity stress

The onset of salinity stress led to a significant shift in  $H^+$  fluxes towards more negative values in all species and both root zones assessed. The magnitude of this shift, however, showed a clear species and tissue dependence (Fig. 5). In the elongation zone, all three species had net initial uptake (zero to 5 min; Fig. 5A). Addition of NaCl led to a shift towards  $H^+$  efflux. This shift was strongest in *B. napus* followed by *B. juncea* and then by *B. oleracea* (Fig. 5A). A similar pattern was also observed in the mature zone (Fig. 5B), although here the steady-state initial  $H^+$  flux values were more negative in all species (net efflux of  $-6 \pm 0.9$   $\text{nmol m}^{-2} \text{s}^{-1}$  in *B. napus* and  $0.2 \pm 1.1$   $\text{nmol m}^{-2} \text{s}^{-1}$  in *B. juncea*, compared with  $\sim 22 \pm 1.8$   $\text{nmol m}^{-2} \text{s}^{-1}$  in both species in the elongation zone. The peak  $H^+$  flux values in the mature zone were  $-30 \pm 4$ ,  $-6 \pm 4$ , and  $-2.5 \pm 2$   $\text{nmol m}^{-2} \text{s}^{-1}$  for *B. napus*, *B. juncea*, and *B. oleracea*, respectively (Fig. 5B), and  $-42 \pm 12$ ,  $-28 \pm 8$ , and  $0 \pm 2$   $\text{nmol m}^{-2} \text{s}^{-1}$  in the elongation zone (Fig. 5A).

The NaCl activation of  $H^+$  pumping was largely prevented by vanadate which reduced  $H^+$  efflux peak values from  $-30 \pm 4$   $\text{nmol m}^{-2} \text{s}^{-1}$  to  $-5 \pm 1$   $\text{nmol m}^{-2} \text{s}^{-1}$  upon vanadate pre-treatment (demonstrated as an example for *B. napus*;

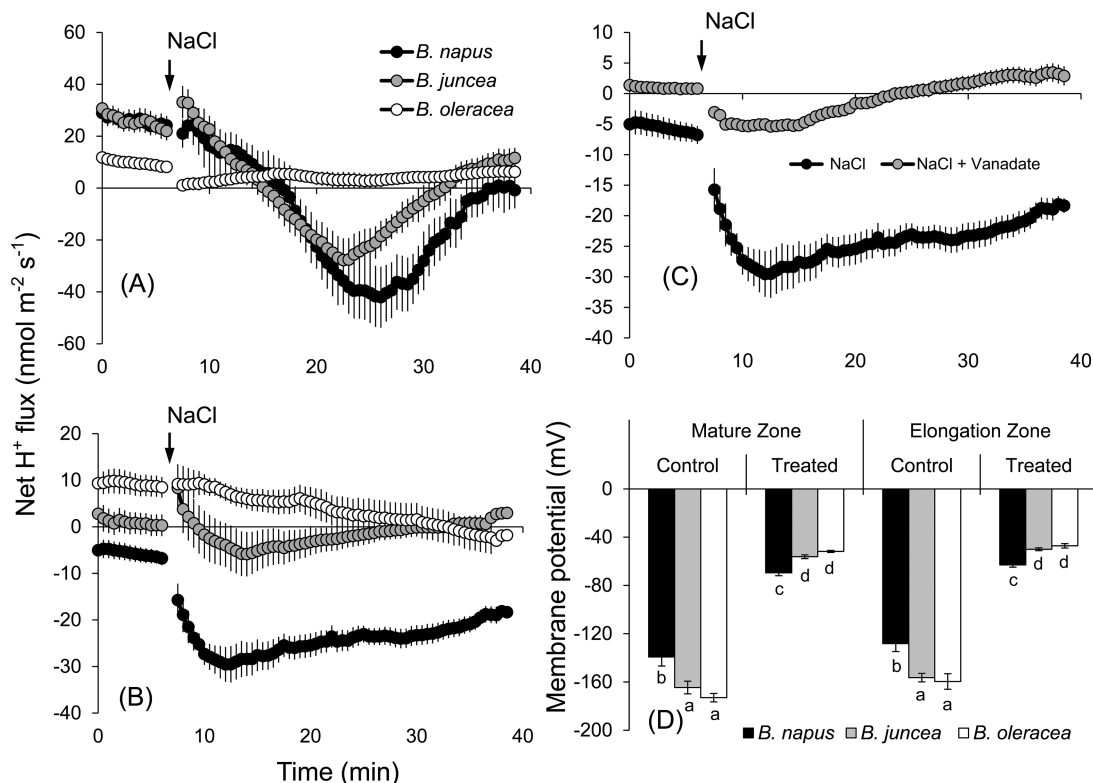


**Fig. 5.** Transient net  $H^+$  flux kinetics measured in three *Brassica* species from elongation (A) and mature (B) root zones in response to 150 mM NaCl stress. (C) Transient net  $H^+$  flux kinetics in response to 150 mM NaCl treatment measured from the mature root zone of *B. napus* pre-treated for 1 h with 1 mM sodium orthovanadate. Values are the mean  $\pm$  SE ( $n=6-8$ ). (D) Membrane potential (mV) of epidermal root cells of three *Brassica* species measured from roots exposed to 150 mM NaCl stress for 48 h. Mean  $\pm$  SE ( $n=20-25$ ).



Fig. 5C). Also affected was the steady-state initial  $H^+$  flux (negative in the control; slightly positive after vanadate pre-treatment). Taken together, these results point towards the involvement of  $H^+$ -ATPase. Given the fact that the plasma membrane  $H^+$ -ATPase is a critical player in determining the MP of plant cells (Palmgren and Niessen, 2011), MP values were tested in three varieties under control and salt treatment (48 h NaCl) conditions. The largest decrease in MP values was observed in *B. oleracea* in both the mature (from  $-170 \pm 4$  mV in control to  $-50 \pm 0.8$  mV after salt treatment) and elongation (from  $-160 \pm 6.5$  to  $-47 \pm 1.8$  mV) zones, respectively (Fig. 5D). *Brassica napus* not only showed the least reduction in MP under long-term salt stress, but also was able to maintain the highest MP under 150 mM salt treatment in both the mature ( $-70 \pm 2.5$  mV) and elongation ( $-63 \pm 1.9$  mV) zones.

#### ROS-induced $K^+$ leakage is related to the active efflux of $Ca^{2+}$ through $Ca^{2+}$ -ATPase

Production of ROS under salinity stress is inevitable, and thus a plant's ability to withstand ROS stress is often associated with the overall salt tolerance (Bose *et al.*, 2014b). To assess the sensitivity of the three *Brassica* species to oxidative stress, the seedlings were subjected to hydroxyl radical generation by Cu/A treatment (Demidchik *et al.* 2003, 2010). Addition of Cu/A to the BSM solution resulted in a profuse  $K^+$  efflux, in both the mature and elongation zones (Fig. 6). The magnitude of this efflux differed significantly between the two zones, with almost a 10-fold higher efflux observed from the

elongation zone. Here, the peak values of  $K^+$  efflux occurred 7–8 min after the treatment (Fig. 6A). In the mature zone, the extent of Cu/A activation of the  $K^+$  efflux was inversely correlated with the overall salinity stress tolerance (*B. oleracea* > *B. juncea* > *B. napus*) (Fig. 6B).

ROS stress is known to affect  $Ca^{2+}$  homeostasis in plants (Demidchik *et al.*, 2010; Zepeda-Jazo *et al.*, 2011), with possible implications for salinity stress signalling. Therefore, we measured the kinetics of net  $Ca^{2+}$  fluxes in response to Cu/A treatment. Of all ROS produced under saline conditions, the hydroxyl radical is the most aggressive and cannot be controlled by means of enzymatic antioxidants (for a review, see Bose *et al.*, 2014b). In addition, due to the signalling role of  $H_2O_2$  in plant adaptive responses (Gilroy *et al.*, 2014; Niu and Liao, 2016; Shabala *et al.*, 2016b), it is often rather difficult to separate 'detrimental' and 'beneficial' effects of  $H_2O_2$  on the activity of ion transporters. Taken together, these two facts determined our use of the hydroxyl radical as a ROS agent in this work. Application of the Cu/A hydroxyl radical-generating mix to *Brassica* roots stimulated net  $Ca^{2+}$  uptake in the elongation zone (Fig. 7A) but resulted in a gradually decaying net  $Ca^{2+}$  efflux from the mature zone (Fig. 7B). No clear differences between species have emerged. Interestingly, immediately upon Cu/A application, a brief transient  $Ca^{2+}$  efflux was also measured in all three *Brassica* species for several minutes, before turning into net  $Ca^{2+}$  uptake (Fig. 7A). Due to the ~100-fold higher  $Ca^{2+}$  concentration gradient

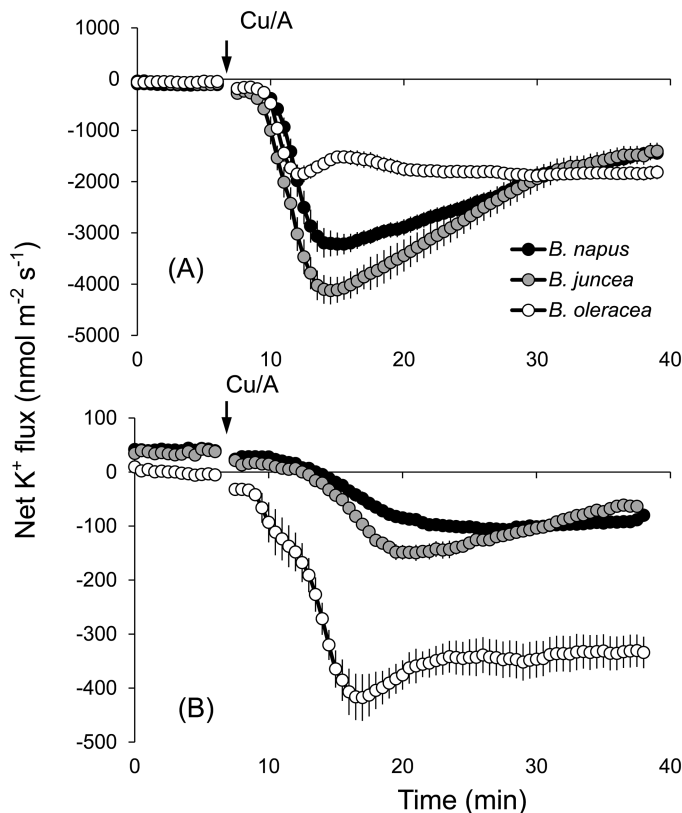


**Fig. 6.** Transient net  $K^+$  flux kinetics measured in three *Brassica* species from the elongation (A) and mature (B) root zones in response to oxidative (1 mM Cu/A) stress. Values are the mean  $\pm$ SE ( $n=4-6$ ).

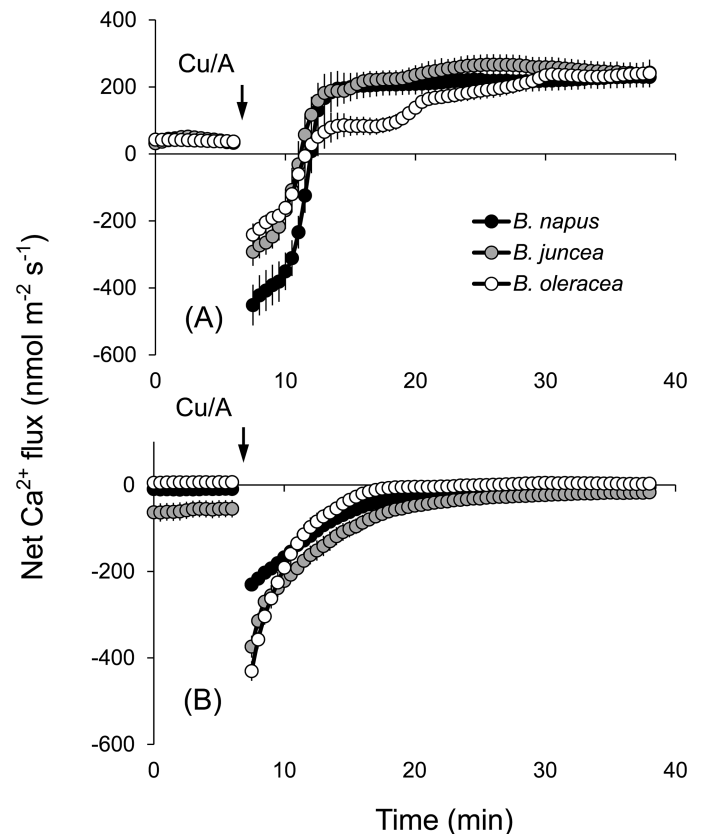


**Fig. 7.** Transient net  $Ca^{2+}$  flux kinetics measured in three *Brassica* species from the elongation (A) and mature (B) root zones in response to oxidative (1 mM Cu/A) stress. Values are the mean  $\pm$ SE ( $n=4-6$ ).



across the plasma membrane, the passive  $\text{Ca}^{2+}$  efflux is thermodynamically impossible and could either originate from the cell wall (as a result of the Donnan exchange; Kinraide, 1998; Shabala and Newman, 2000) or be mediated by some active plasma membrane  $\text{Ca}^{2+}$  efflux system. To differentiate between these two possible sources, we pre-treated roots with Eosin Yellow (EY), a known inhibitor of  $\text{Ca}^{2+}$ -ATPase (Romani *et al.*, 2004; Beffagna *et al.*, 2005). Pre-treatment of *B. napus* roots with EY completely blocked the initial  $\text{Ca}^{2+}$  efflux, suggesting involvement of Ca-ATPase in active  $\text{Ca}^{2+}$  pumping out from the cells (Fig. 7C). EY was also found to shorten the timing of the response to Cu/A, with the peak  $\text{K}^+$  efflux in the presence of EY occurring 3 min prior to the peak values without EY in the elongation zone (Fig. 8A), and exacerbated the extent of Cu/A-induced activation of net  $\text{K}^+$  efflux from the mature zone (Fig. 8B).

#### Selective induction of key ion transporters/pumps in *B. napus* explains its higher salinity tolerance among Brassica species

Quantitative real-time PCR analyses were carried out to assess the relative abundance of the transcript level in control (0h) and after short-term (1 h) and long-term (48 h) salt stress in the three *Brassica* species. As postulated from the ion flux data and pharmacological tests, we found a significant induction of the plasma membrane  $\text{Na}^+/\text{H}^+$ -antiporter (*SOS1*) transcript in *B. napus*, after both 1 h and 48 h of 150 mM salt treatment. The relative induction of *SOS1* transcript was ~5.5- and ~7-fold after 1 h and 48 h from the onset of salt stress, respectively (Fig. 9A), while it was induced

only marginally in *B. juncea* (1.4- and 1.8-fold induction 1 h and 48 h after salt treatment, respectively). In the case of *B. oleracea*, the transcript level was not increased 1 h after the treatment, while it was increased slightly (~1.4-fold) 48 h afterwards. Upon exposure to salt stress, the transcript level of the plasma membrane  $\text{H}^+$ -ATPase (*AHA1*) was also induced sharply only in *B. napus* (3.7- and 10-fold induction 1 h and 48 h after onset of the stress, respectively) (Fig. 9B). Neither *B. juncea* nor *B. oleracea* showed any significant ( $P < 0.05$ ) up-regulation of the *AHA1* transcript. Unlike *SOS1* and *AHA1* genes, the expression of the *Ca-ATPase* gene did not show a continuous increasing pattern with the increase of the salt treatment period (Fig. 9C). The highest induction of the *Ca-ATPase* transcript was observed in *B. napus*, 1 h after the salt treatment (~10-fold), which decreased after 48 h salt treatment (compared with 1 h treatment) while still remaining ~3-fold higher than the control value. The minimal induction of *Ca-ATPase* transcript was observed in *B. juncea*, that was not statistically significant.

The expression patterns of other key cellular ion transporters mediating intracellular  $\text{K}^+$  and  $\text{Na}^+$  homeostasis were also investigated (Fig. 10). Our first candidate was the GORK channel that mediates salt stress-induced  $\text{K}^+$  efflux from the cell in many plant species (Shabala and Cuin, 2008; Shabala and Pottosin, 2014). Salinity stress induced *GORK* transcript levels in all three *Brassica* species, in a time-dependent manner (Fig. 10A). After 1 h of salt stress, there was no induction of *GORK* observed in *B. napus*, while there was a >2.5-fold induction in both *B. juncea* and *B. oleracea* (Fig. 10A). Although 48 h of NaCl stress led to significant induction in *GORK* transcript abundance even in *B. napus*, the magnitude of induction

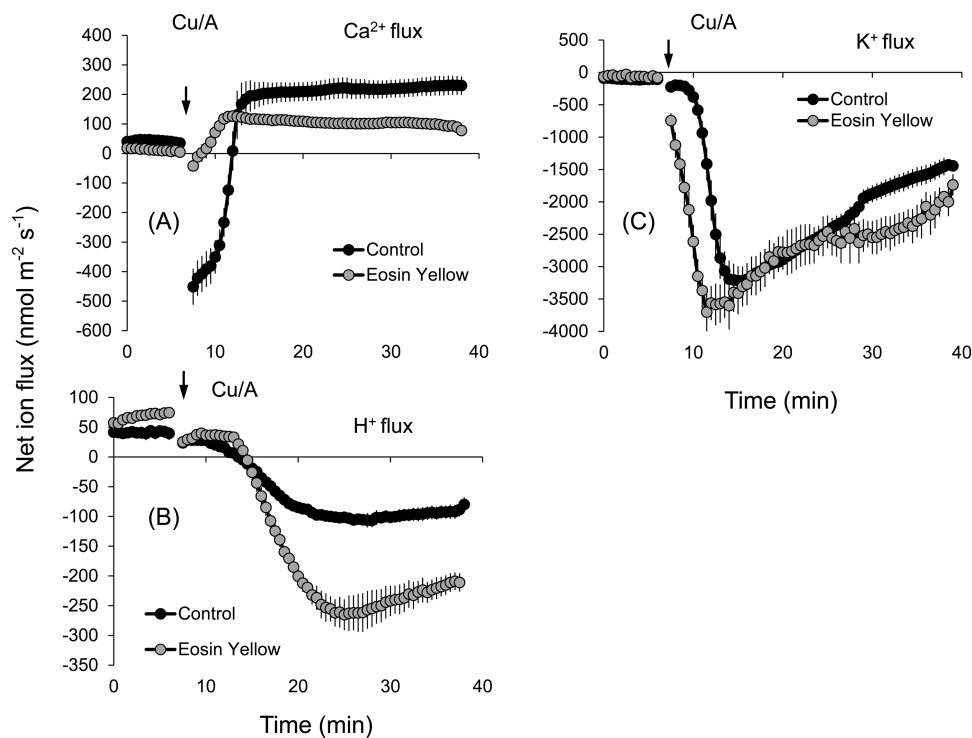


**Fig. 8.** Transient net  $\text{Ca}^{2+}$  (A),  $\text{H}^+$  (B), and  $\text{K}^+$  (C) flux kinetics measured in response to oxidative (1 mM Cu/A) stress from the elongation root zone of *B. napus* pre-treated for 1 h in solutions containing 1  $\mu\text{M}$  Eosin Yellow, a known blocker of the  $\text{Ca}^{2+}$ -ATPase pump. Values are the mean  $\pm$ SE ( $n=4-6$ ).

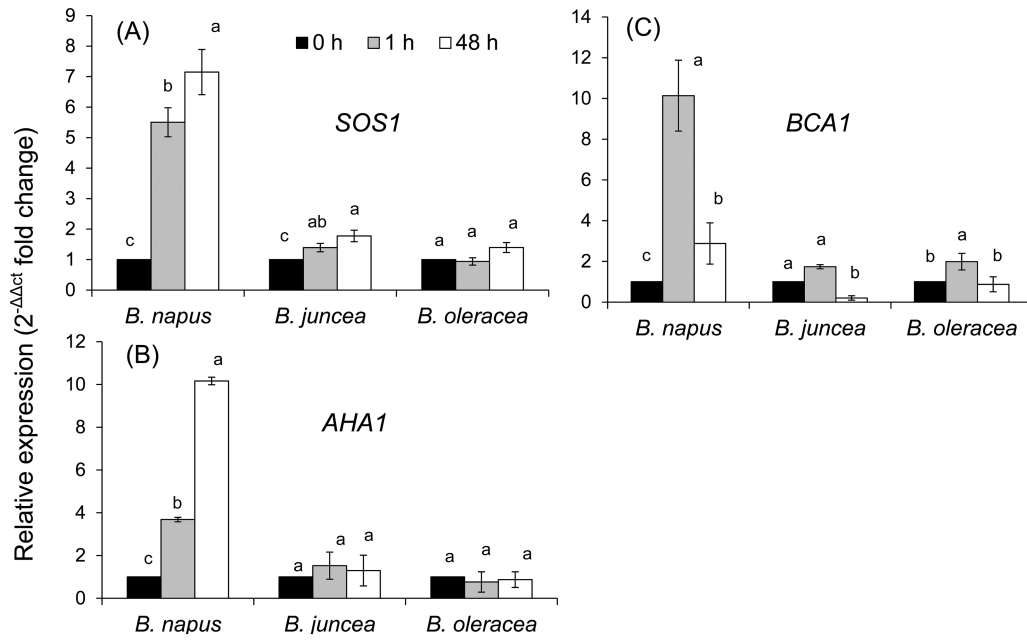


**Fig. 9.** Quantitative real-time PCR analysis of the time-dependent expression pattern of *SOS1* (A), *AHA1* (B), and *BCA1* (C) genes in roots of three *Brassica* species grown in non-buffered basic salt medium (BSM) solution (0.5 mM KCl+0.2 mM NaCl+0.1 mM CaCl<sub>2</sub>, pH 5.7) and exposed to 150 mM NaCl stress for 0, 1, and 48 h. The total RNA was extracted collectively from at least five individual plants for each treatment combination. Values are the mean  $\pm$  SE ( $n=6$  independent real-time PCRs performed). The relative fold-change values are given as the mean  $\pm$  SE in each case.

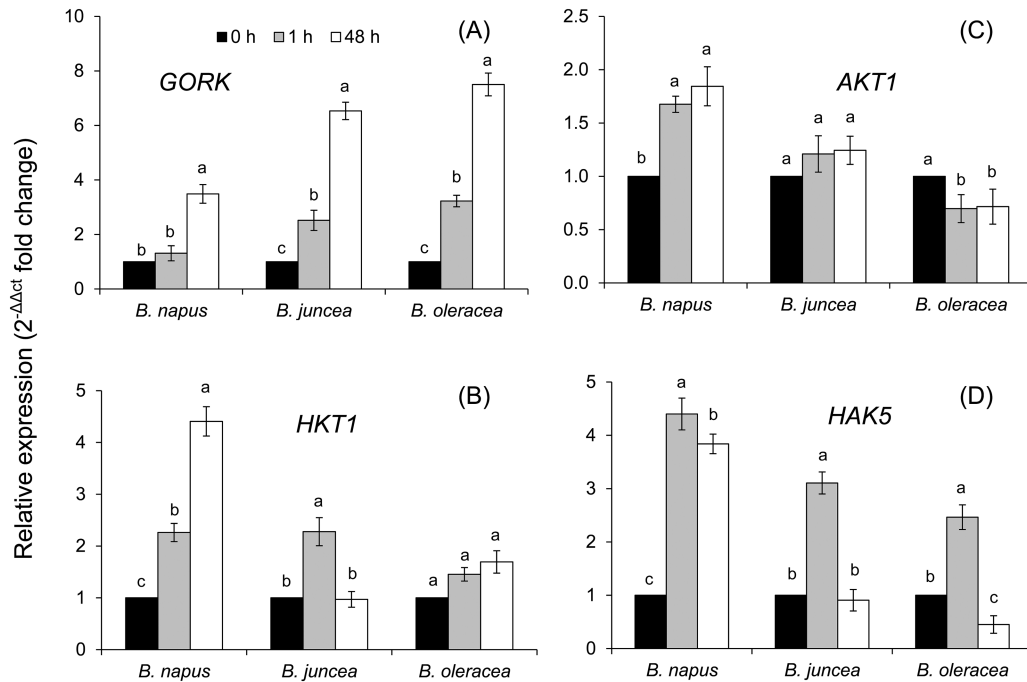


**Fig. 10.** Quantitative real-time PCR analysis of the time-dependent expression pattern of *GORK* (A), *HKT1* (B), *AKT1* (C), and *HAK5* (D) genes in roots of three *Brassica* species grown in non-buffered basic salt medium (BSM) solution (0.5 mM KCl+0.2 mM NaCl+0.1 mM CaCl<sub>2</sub>, pH 5.7) and exposed to 150 mM NaCl stress for 0, 1, and 48 h. The total RNA was extracted collectively from at least five individual plants for each treatment combination. Values are the mean  $\pm$  SE ( $n=6-9$  independent real-time PCRs performed). The relative fold-change values are given as the mean  $\pm$  SE in each case.

was  $\sim$ 2-fold lower compared with the other two species. The quantitative PCR data on the relative transcript abundance of *HKT1*, *AKT1*, and *HAK5* showed a comparatively higher level of induction in *B. napus* for all three genes (Fig. 10B–D). In fact, the *AKT1* transcript did not show any significant change in either *B. juncea* or *B. oleracea* upon exposure to salt stress, while *HKT1* showed induction upon 1 h of salt exposure in *B. juncea*,

but no significant induction in *B. oleracea*. Strong up-regulation (although with differential magnitude) of the *HAK5* transcript was observed in all three *Brassica* species with short-term salt stress (1 h), but it was either decreased to the initial level or even down-regulated with a longer duration (48 h) of stress, except in *B. napus*, which was able to maintain  $\sim$ 3.8-fold up-regulation of the *HAK5* transcript level even after 48 h of stress.

## Discussion

Similar to other cultivated glycophyte species, *Brassica* are also sensitive to salinity stress and possess a certain degree of variability in salinity tolerance at the species level (Ashraf *et al.*, 2001; Kumar *et al.*, 2009). Genetically, such variability in salt tolerance in *Brassica* is thought to be associated with the ploidy level of the species (Ashraf and McNeilly, 2004). In the present study, we found distinctive differences in salt tolerance of the three *Brassica* species studied. The root growth assay suggested the order of salt tolerance as *B. napus* > *B. juncea* > *B. oleracea* (Fig. 1); this was further confirmed by the viability staining data (Fig. 2). While these findings are consistent with some previous observations (Ashraf *et al.*, 2001; Purty *et al.*, 2008), no explanation for this intraspecific differential sensitivity to salt was given until now, at the mechanistic level. Here we provide strong evidence that higher salt tolerance in *B. napus* is conferred by at least three complementary physiological mechanisms: (i) higher Na<sup>+</sup> extrusion ability from roots resulting from increased expression and activity of plasma membrane SOS1-like Na<sup>+</sup>/H<sup>+</sup> exchangers; (ii) better root K<sup>+</sup> retention ability resulting from stress-inducible activation of H<sup>+</sup>-ATPase and the ability to maintain a more negative MP under saline conditions; and (iii) reduced sensitivity of *B. napus* root K<sup>+</sup>-permeable channels to ROS. Of these, the two latter mechanisms played the dominant role in conferring salinity stress tolerance in *Brassica*. The supporting arguments are given below.

### *SOS1-mediated Na<sup>+</sup> extrusion may be essential for higher salt tolerance in B. napus*

A massive influx of Na<sup>+</sup> was observed in all three *Brassica* species immediately after imposition of salinity stress. Given the strong cytotoxicity of Na<sup>+</sup> (Munns and Gilliham, 2015), plant performance under saline conditions will be critically dependent on the ability of *Brassica* species to remove excessive Na<sup>+</sup> from the cytosol, either to the external media or by sequestering it into the vacuole. In contrast to mammalian systems, higher plants do not harbour Na<sup>+</sup> ATPase pumps (Maathuis, 2014), and the above exclusion is believed to be mediated by Na<sup>+</sup>/H<sup>+</sup> exchangers [either SOS1 at the plasma membrane (Shi *et al.*, 2000) or NHX at the tonoplast membrane (Blumwald *et al.*, 2000)]. Here we provide strong evidence that superior salinity stress tolerance in *B. napus* is conferred by higher SOS1 activity. Indeed, *B. napus* was the only species showing active Na<sup>+</sup> exclusion in both the mature and elongation root zones (Fig. 3A, B). This Na<sup>+</sup> efflux was found to be sensitive to both vanadate (a known inhibitor of H<sup>+</sup>-ATPase that provides a driving force for Na<sup>+</sup>/H<sup>+</sup> antiporter operation) and amiloride [a known blocker of Na<sup>+</sup>/H<sup>+</sup> exchangers in both mammalian (Grinstein *et al.* 1988) and plant (Cuin *et al.*, 2011) systems] (Fig. 3D), strongly suggesting the involvement of SOS1. This is further confirmed by measuring stress-induced changes in SOS1 transcript levels (Fig. 9) that were several fold greater in *B. napus* compared with the two other *Brassica* species. Also strongly induced was AHA1 expression (a 10-fold increase in transcript level),

conferring the possibility to fuel the SOS1 operation. Thus, it is plausible to suggest that *B. napus* possesses a very efficient salt-sensing system that is able to translate changes in the rhizosphere conditions into both transcriptional (Fig. 9) and functional (Fig. 3) changes in the SOS1 activity. Specific details of the mechanisms behind the observed activation remain obscure. Zhu (2003) has argued that SOS1 protein has a long tail that resides in the cytoplasm and, by analogy with bacterial and yeast systems, may potentially operate as a Na<sup>+</sup> sensor *per se*. However, no direct experimental support for this hypothesis has been provided so far, and it was argued (Shabala *et al.*, 2015) that SOS1 activity is regulated by a SOS3/SOS2 complex, which activates its C-terminus from the cytosolic site and thus relies on changes in cytosolic free Ca<sup>2+</sup> (not external Na<sup>+</sup>) concentrations. Given the fact that changes in SOS1 activity strongly correlated with changes in net K<sup>+</sup> and H<sup>+</sup> fluxes, involvement of the H<sup>+</sup>-ATPase/GORK tandem system as a potential Na<sup>+</sup> sensor (Shabala *et al.*, 2015) may be plausible. This issue is discussed in more detail in the following sections. It should be also noted that net Na<sup>+</sup> efflux was not observed in either the elongation or the mature zone of the other two *Brassica* species (Fig. 3C), and thus cannot be responsible for the reported higher tolerance of *B. juncea* as compared with *B. oleracea* (Figs 1, 2). Thus, it is suggested that Na<sup>+</sup> exclusion from uptake plays an important but not a crucial role as a determinant of genetic variability in salinity stress tolerance in *Brassica*.

### *Maintenance of K<sup>+</sup> homeostasis is critical for salt tolerance in B. napus*

Maintenance of K<sup>+</sup> homeostasis is essential for enzyme activities, ionic and pH homeostasis, and charge balance (Dreyer and Uozumi, 2011), and cytosolic K<sup>+</sup> is considered to be the common denominator of plant adaptive responses to a broad range of environmental stresses (Shabala and Pottosin, 2014; Shabala *et al.*, 2016a). Changes in the cytosolic K<sup>+</sup> are also suggested to be an important signal that may determine the cell's fate and also switch its operation from the metabolic to defence mode (Demidchik *et al.*, 2014). Both X-ray crystallographic and ion-selective microelectrode-based measurements of the cytosolic K<sup>+</sup> level were shown to be decreased considerably under salinity stress (Flowers and Hajibagheri, 2001; Cuin *et al.*, 2003), and a strong correlation between the root's K<sup>+</sup> retention ability and plant salinity stress tolerance was reported for several species including wheat (Cuin *et al.*, 2008, 2012), barley (Chen *et al.*, 2005, 2007; Wu *et al.*, 2015), poplar (Sun *et al.*, 2009), and lucerne (Smethurst *et al.*, 2008). Here we extend this list and show that the above mechanism is also applicable to explain the intraspecific variability in salinity tolerance in *Brassica*. Indeed, the average total K<sup>+</sup> leak was found to be in the order *B. napus* < *B. juncea* < *B. oleracea*, which was in an agreement with the overall ability of these species to tolerate external salt stress (Fig. 4). A strong correlation (see Supplementary Table S3) between K<sup>+</sup> retention and net Na<sup>+</sup> uptake observed in the *Brassica* species (especially in the mature root zone); sensitivity of NaCl-induced K<sup>+</sup> efflux to vanadate and amiloride (Fig. 4D); and a positive correlation

between root  $K^+$  retention ability and plasma membrane potential under saline conditions (Fig. 5D) collectively point towards involvement of GORK channels as a major pathway for the salt stress-induced  $K^+$  efflux from *Brassica* roots. GORK (outward-rectifying potassium selective) channels are activated by membrane depolarization (Very *et al.*, 2014), and their gating is strongly dependent upon the extracellular  $K^+$  concentration (Anschutz *et al.*, 2014). GORK channels are ubiquitously expressed in Arabidopsis tissues and represent an essential element in volume control of various cell types such as guard cells, pollen tube, or root hairs (Becker *et al.*, 2003; Hosy *et al.*, 2003). They are also known to be ROS sensitive and determine cell fate by mediating induction of programmed cell death under saline conditions (Demidchik *et al.*, 2010). These findings reported for Arabidopsis are in a very good agreement with our data reporting much smaller activation of  $K^+$  efflux by the hydroxyl radical-generating Cu/A mix in *B. napus* roots (Fig. 6B) compared with the two other species. Thus, it may be concluded that the intraspecific variability in salinity stress tolerance among *Brassica* species is critically dependent on the functional expression and/or regulation of GORK channels under saline conditions.

Interestingly, *GORK* transcript levels were up-regulated by 4- to 7-fold, in a clear time-dependent manner (Fig. 10A). This is counterintuitive and contradicts the above notion of the essentiality of  $K^+$  retention in salinity stress tolerance. The most likely explanation is the comment made above that plants may use  $K^+$  efflux as a switch from metabolic to defence mode (Demidchik *et al.*, 2014), and increased expression of GORK channels may assist plants in achieving this goal. As such a switch has a caveat of losing too much  $K^+$ , a very fine balance between the amount of  $K^+$  lost in this signalling process and the amount of  $K^+$  retained in the root for turgor and/or metabolic purposes is needed. *Brassica napus* plants seem to be very efficient in maintaining such a balance. Not only is the reported increase in *GORK* transcript 2-fold lower in *B. napus* compared with the other two species, but *B. napus* plants showed much higher transcript levels of both low (*AKT1*) and high (*HAK5*) affinity transport systems involved in  $K^+$  acquisition (hence, restoring cytosolic  $K^+$  levels once the signalling is over). Also 2- to 3-fold higher were the *HKT1* transcript levels in *B. napus* 48 h after stress onset (Fig. 10B). Traditionally, the role of *HKT1* is attributed to retrieval of  $Na^+$  from the xylem (Munns and Tester, 2008). This suggests a better  $Na^+$  retention in the root of *B. napus* and a potential for its use for osmotic (turgor maintenance) purposes, to compensate for  $K^+$  lost.

*Maintenance of a higher membrane potential under salinity stress is achieved by an active  $H^+$  pumping by B. napus*

An active  $H^+$  pumping is the key to maintaining the negative MP required for optimal plant growth (Sze *et al.*, 1999). Under saline conditions, NaCl induces activation of both plasma membrane and vacuolar  $H^+$ -ATPases that are required to restore the otherwise depolarized MP in both halophytes and glycophytes (Yang *et al.*, 2007; Bose *et al.*, 2015). Here

we show that the differential sensitivity of *Brassica* species to salinity stress is determined by the extent of NaCl-induced activation of  $H^+$ -ATPase, at both the transcriptional (Fig. 9) and post-translational (Fig. 5) level.

A significant correlation between membrane depolarization and  $K^+$  leakage from the root tissue was established in earlier reports (Chen *et al.*, 2007; Bose *et al.*, 2014a) and attributed to the depolarization-activated outward-rectifying  $K^+$  channels (Shabala and Pottosin, 2014). In agreement with this, a dramatic  $K^+$  efflux was observed in all *Brassica* species tested (Fig. 4) that correlated with the extent of MP depolarization (Fig. 5). The NaCl-induced  $H^+$  efflux was almost instantaneous (Fig. 5B) and strongly blocked by vanadate, a known inhibitor of  $H^+$ -ATPase (Fig. 5C). The causal link between the cytosolic  $K^+$  concentration and  $H^+$ -ATPase activity was suggested by Buch-Pedersen *et al.* (2006) who showed that the plant plasma membrane  $H^+$ -ATPase is regulated by potassium bound to the proton pump at a site involving Asp617 in the cytoplasmic phosphorylation domain, suggesting a role for  $K^+$  as an intrinsic uncoupler. Thus, it was suggested that GORK channels may be located in close proximity to  $H^+$ -ATPase, forming a 'microdomain' in the lipid raft (Shabala *et al.*, 2015), and that a reduction in the cytosolic  $K^+$  concentration in the  $H^+$ -ATPase microdomain may affect operation of the  $H^+$  pump as described above. This GORK/ $H^+$ -ATPase 'tandem' may then operate as a salt sensor and explain the differential sensitivity between *Brassica* species.

*Differential ROS sensitivity in salt stress signalling in Brassica*

Plants growing in a saline environment are facing cytotoxic ROS produced as a secondary effect of salinity stress. Demidchik *et al.* (2010) reported a 2.5- to 3-fold increase in hydroxyl radicals in Arabidopsis roots exposed to 100mM NaCl stress. Also the amount of  $H_2O_2$  accumulated in the roots showed a significant increase under salt stress (Xie *et al.*, 2011). This increased load of ROS under saline conditions was shown to activate GORK channels, which conduct large outwardly rectifying  $K^+$  currents and thus increase  $K^+$  leakage from the tissue (Demidchik *et al.*, 2010). In full agreement with this, we report a high degree of  $K^+$  leakage in the mature zone of all three *Brassica* as soon as they are exposed to oxidative stress (Fig. 6B). The most salt-sensitive species, *B. oleracea*, not only showed the highest  $K^+$  efflux but the rate of induction of  $K^+$  leakage was also much faster in this species (judged by the timing of peak  $K^+$  efflux). Overall,  $K^+$  retention capacity in the mature root zone under oxidative stress (imposed by the hydroxyl radical-generating Cu/A mix; Demidchik *et al.*, 2003) was *B. napus*>*B. juncea*>*B. oleracea* as the order of tolerance, which is similar to the respective order for root growth and root viability under salt stress (Figs 1, 2). Interestingly, the pattern of  $K^+$  efflux was not similar in the elongation zone (Fig. 6A). In fact, it was almost the other way around, with *B. juncea* and *B. napus* showing higher  $K^+$  efflux than *B. oleracea*. Again, it may be tempting to suggest, therefore, that ROS-induced  $K^+$  leak from the root apex may perform a 'positive' (signalling) role, either switching



cell metabolism from the metabolic into defence mode of operation (Demidchik *et al.*, 2014), thus enabling a rapid plant adaptation to altered conditions in the rhizosphere, or initiating a long-distance (root to shoot) signalling cascade (Shabala *et al.*, 2016b).

Oxidative stress is known also to affect  $\text{Ca}^{2+}$  homeostasis (Demidchik *et al.*, 2003) through a large number of  $\text{Ca}^{2+}$  transport systems (Demidchik *et al.*, 2010; Zepeda-Jazo *et al.*, 2011). Accordingly, ROS-induced net  $\text{Ca}^{2+}$  fluxes were also measured and assessed in this work. A rapid initial efflux of  $\text{Ca}^{2+}$  was observed from both the mature and elongation zones of *Brassica* roots immediately upon exposure to the oxidative stress (Fig. 7A, B). In the elongation zone, the highest  $\text{Ca}^{2+}$  efflux was observed in *B. napus*, which was converted into steady uptake of  $\text{Ca}^{2+}$  7–12 min after the stress application. For the other two species, the trend was also similar, with a slight difference between the periods of efflux in these species. As passive (channel-mediated)  $\text{Ca}^{2+}$  efflux is thermodynamically not possible, the reported data suggest a rapid activation by ROS of some active  $\text{Ca}^{2+}$  efflux systems, which is more pronounced in the salt-tolerant *B. napus* species. Cellular membranes harbour a large number of  $\text{Ca}^{2+}$  efflux systems ( $\text{Ca}^{2+}$ -ATPase family) and  $\text{Ca}^{2+}$  exchangers (CAX family) (McAinsh and Pittman, 2009; Bose *et al.*, 2011), and activation of plasma membrane-based  $\text{Ca}^{2+}$ -ATPase pumps by hydroxyl radicals was demonstrated in pharmacological and patch-clamp experiments in pea root cells (Zepeda-Jazo *et al.*, 2011). Accordingly, we have hypothesized that a similar scenario may be applicable to *Brassica* roots. Pharmacological tests revealed that the ROS-induced  $\text{Ca}^{2+}$  efflux was sensitive to EY, a known blocker of  $\text{Ca}^{2+}$ -ATPase. The activation of  $\text{Ca}^{2+}$ -ATPase also happened to be the highest in the elongation zone of *B. napus* and the lowest in the mature zone of *B. napus*, suggesting tissue-specific  $\text{Ca}^{2+}$  signalling in this species. The observed efflux is transient and is gradually transformed into net  $\text{Ca}^{2+}$  uptake that most probably results from the hydroxyl radical-induced activation of  $\text{Ca}^{2+}$ -permeable channels in root plasma membranes, as reported in direct patch-clamp experiments on other species (Demidchik *et al.*, 2003; Foreman *et al.*, 2003; Demidchik and Maathuis, 2007; Zepeda-Jazo *et al.*, 2011). Taken together, a concurrent (or very closely timed) activation of both  $\text{Ca}^{2+}$  efflux and  $\text{Ca}^{2+}$  influx systems may shape the cytosolic  $\text{Ca}^{2+}$  signature, conferring specificity of the stress signal (Knight and Knight, 2001; Demidchik *et al.*, 2002; Ludwig *et al.*, 2004; Demidchik and Maathuis, 2007; Dodd *et al.*, 2010). Consistent with this suggestion were changes in BCA1 transcript levels that peaked at 1 h and declined afterwards (once the signalling was over). The reported induction in BCA1 transcript was significantly higher in *B. napus* (Fig. 9C), consistent with the reported strongest net  $\text{Ca}^{2+}$  efflux from its roots (Fig. 7A).

## Conclusions

To summarize, the superior salinity stress tolerance of *B. napus* was conferred by its better ability to exclude  $\text{Na}^+$  and retain  $\text{K}^+$ , thus providing an optimal cytosolic K/Na ratio.

This ability was determined by the efficient transcriptional and post-translational regulation of key transport systems, namely the plasma membrane  $\text{H}^+$ -ATPase pump, the SOS1  $\text{Na}^+/\text{H}^+$  exchanger, P-type  $\text{Ca}^{2+}$ -ATPase, and low- and high-affinity  $\text{K}^+$  uptake systems. Specific details of their regulation and salt stress perception and signalling pathways remain to be revealed in follow-up studies.

## Supplementary data

Supplementary data are available at *JXB* online.

**Figure S1.** Propidium iodide-stained *B. oleracea* root apex showing dead cells after 48 h of 150 mM NaCl stress.

**Table S1.** List of liquid ionophores and respective back-filling solution used for micro-electrode preparation.

**Table S2.** Nucleotide sequences of different primers used in the study along with amplicon length.

**Table S3.** Correlation matrix (two-tailed Pearson's correlation) for different physiological and ion uptake parameters with transcript abundance of key transporters/proteins

## Acknowledgements

This work has been supported by an Endeavour Research Fellowship, Australia Awards, Australian Government Department of Education to KC, and Australian Research Council and Grain Research and Development Corporation grants to SS.

## References

- Adem GD, Roy SJ, Zhou M, Bowman JP, Shabala S. 2014. Evaluating contribution of ionic, osmotic and oxidative stress components towards salinity tolerance in barley. *BMC Plant Biology* **14**, 113.
- Anschütz U, Becker D, Shabala S. 2014. Going beyond nutrition: regulation of potassium homeostasis as a common denominator of plant adaptive responses to environment. *Journal of Plant Physiology* **171**, 670–687.
- Ashraf M, Athar HR, Harris PJC, Kwon TR. 2008. Some prospective strategies for improving crop salt tolerance. *Advances in Agronomy* **97**, 45–110.
- Ashraf M, McNeilly T. 2004. Salinity tolerance in *Brassica* oilseeds. *Critical Reviews in Plant Science* **23**, 157–174.
- Ashraf M, Nazir N, McNeilly T. 2001. Comparative salt tolerance of amphidiploid and diploid *Brassica* species. *Plant Science* **160**, 683–689.
- Becker D, Hoth S, Ache P, Wenkel S, Roelfsema MR, Meyerhoff O, Hartung W, Hedrich R. 2003. Regulation of the ABA-sensitive *Arabidopsis* potassium channel membrane  $\text{H}^+$ -ATPase and  $\text{H}^+$ -ATPase. *FEBS Letters* **554**, 119–126.
- Beffagna N, Buffoli B, Busi C. 2005. Modulation of reactive oxygen species production during osmotic stress in *Arabidopsis thaliana* cultured cells: involvement of the plasma membrane  $\text{Ca}^{2+}$ -ATPase and  $\text{H}^+$ -ATPase. *Plant and Cell Physiology* **46**, 1326–1339.
- Blumwald E, Aharon GS, Apse MP. 2000. Sodium transport in plant cells. *Biochimica et Biophysica Acta* **1465**, 140–151.
- Bose J, Pottosin II, Shabala SS, Palmgren MG, Shabala S. 2011. Calcium efflux systems in stress signaling and adaptation in plants. *Frontiers in Plant Science* **2**, 85.
- Bose J, Rodrigo-Moreno A, Lai D, Xie Y, Shen W, Shabala S. 2015. Rapid regulation of the plasma membrane  $\text{H}^+$ -ATPase activity is essential to salinity tolerance in two halophyte species, *Atriplex lentiformis* and *Chenopodium quinoa*. *Annals of Botany* **115**, 481–494.
- Bose J, Rodrigo-Moreno A, Shabala S. 2014b. ROS homeostasis in halophytes in the context of salinity stress tolerance. *Journal of Experimental Botany* **65**, 1241–1257.

- Bose J, Shabala L, Pottosin I, Zeng F, Velarde-Buendía A, Massart A, Poschenrieder C, Hariadi Y, Shabala S.** 2014a. Kinetics of xylem loading, membrane potential maintenance, and sensitivity of K<sup>+</sup>-permeable channels to reactive oxygen species: physiological traits that differentiate salinity tolerance between pea and barley. *Plant, Cell and Environment* **37**, 589–600.
- Buch-Pedersen MJ, Rudashevskaya EL, Berner TS, Venema K, Palmgren MG.** 2006. Potassium as an intrinsic uncoupler of the plasma membrane H<sup>+</sup>-ATPase. *Journal of Biological Chemistry* **281**, 38285–38292.
- Chakraborty K, Bose J, Shabala L, Eyles A, Shabala S.** 2016b. Evaluating relative contribution of osmo- and tissue-tolerance mechanisms towards salinity stress tolerance in three Brassica species. *Physiologia Plantarum*. doi:10.1111/ppl.12447.
- Chakraborty K, Sairam RK, Bhaduri D.** 2016a. Effects of different levels of soil salinity on yield attributes, accumulation of nitrogen, and micronutrients in *Brassica* spp. *Journal of Plant Nutrition* **39**, 1026–1037.
- Chakraborty K, Sairam RK, Bhattacharya RC.** 2012. Salinity induced expression of pyrroline-5-carboxylate synthetase determine salinity tolerance in *Brassica* spp. *Acta Physiologiae Plantarum* **34**, 1935–1941.
- Chen Z, Newman I, Zhou M, Mendham N, Zhang G, Shabala S.** 2005. Screening plants for salt tolerance by measuring K<sup>+</sup> flux: a case study for barley. *Plant, Cell and Environment* **28**, 1230–1246.
- Chen Z, Pottosin I, Cuin TA, et al.** 2007. Root plasma membrane transporters controlling K<sup>+</sup>/Na<sup>+</sup> homeostasis in salt-stressed barley. *Plant Physiology* **145**, 1714–1725.
- Chen Z, Shabala S, Mendham N, Newman I, Zhang G, Zhou M.** 2008. Combining ability of salinity tolerance on the basis of NaCl-induced K flux from roots of barley. *Crop Science* **48**, 1382–1388.
- Cuin TA, Betts SA, Chalmandrier R, Shabala S.** 2008. A root's ability to retain K<sup>+</sup> correlates with salt tolerance in wheat. *Journal of Experimental Botany* **59**, 2697–2706.
- Cuin TA, Bose J, Stefano G, Jha D, Tester M, Mancuso S, Shabala S.** 2011. Assessing the role of root plasma membrane and tonoplast Na<sup>+</sup>/H<sup>+</sup> exchangers in salinity tolerance in wheat: in planta quantification methods. *Plant, Cell and Environment* **34**, 947–961.
- Cuin TA, Miller AJ, Laurie SA, Leigh RA.** 2003. Potassium activities in cell compartments of salt-grown barley leaves. *Journal of Experimental Botany* **54**, 657–661.
- Cuin TA, Tian Y, Betts SA, Chalmandrier R, Shabala S.** 2009. Ionic relations and osmotic adjustment in durum and bread wheat under saline conditions. *Functional Plant Biology* **36**, 1110–1119.
- Cuin TA, Zhou M, Parsons D, Shabala S.** 2012. Genetic behaviour of physiological traits conferring cytosolic K<sup>+</sup>/Na<sup>+</sup> homeostasis in wheat. *Plant Biology* **14**, 438–446.
- Davenport R, James RA, Zakrisson-Plogander A, Tester M, Munns R.** 2005. Control of sodium transport in durum wheat. *Plant Physiology* **137**, 807–818.
- Demidchik V.** 2015. Mechanisms of oxidative stress in plants: from classical chemistry to cell biology. *Environmental and Experimental Botany* **109**, 212–228.
- Demidchik V, Cuin TA, Svistunenko D, Smith SJ, Miller AJ, Shabala S, Sokolik A, Yurin V.** 2010. Arabidopsis root K<sup>+</sup>-efflux conductance activated by hydroxyl radicals: single-channel properties, genetic basis and involvement in stress-induced cell death. *Journal of Cell Science* **123**, 1468–1479.
- Demidchik V, Davenport RJ, Tester M.** 2002. Nonselective cation channels in plants. *Annual Review of Plant Biology* **53**, 67–107.
- Demidchik V, Maathuis FJM.** 2007. Physiological roles of nonselective cation channels in plants: from salt stress to signalling and development. *New Phytologist* **175**, 387–404.
- Demidchik V, Shabala SN, Coutts KB, Tester MA, Davies JM.** 2003. Free oxygen radicals regulate plasma membrane Ca<sup>2+</sup>- and K<sup>+</sup>-permeable channels in plant root cells. *Journal of Cell Science* **116**, 81–88.
- Demidchik V, Shabala SN, Davies JM.** 2007. Spatial variation in H<sub>2</sub>O<sub>2</sub> response of *Arabidopsis thaliana* root epidermal Ca<sup>2+</sup> flux and plasma membrane Ca<sup>2+</sup> channels. *The Plant Journal* **49**, 377–386.
- Demidchik V, Straltsova D, Medvedev SS, Pozhvanov GA, Sokolik A, Yurin V.** 2014. Stress-induced electrolyte leakage: the role of K<sup>+</sup>-permeable channels and involvement in programmed cell death and metabolic adjustment. *Journal of Experimental Botany* **65**, 1259–1270.
- Demidchik V, Tester M.** 2002. Sodium fluxes through nonselective cation channels in the plasma membrane of protoplasts from *Arabidopsis* roots. *Plant Physiology* **128**, 379–387.
- Dodd AN, Kudla J, Sanders D.** 2010. The language of calcium signaling. *Annual Review of Plant Biology* **61**, 593–620.
- Dreyer I, Uozumi N.** 2011. Potassium channels in plant cells. *FEBS Journal* **278**, 4293–4303.
- Fan W, Deng G, Wang H, Zhang H, Zhang P.** 2015. Elevated compartmentalization of Na<sup>+</sup> into vacuoles improves salt and cold stress tolerance in sweet potato (*Ipomoea batatas*). *Physiologia Plantarum* **154**, 560–571.
- Flowers TJ, Hajibagheri MA.** 2001. Salinity tolerance in *Hordeum vulgare*: ion concentrations in root cells of cultivars differing in salt tolerance. *Plant and Soil* **231**, 1–9.
- Foreman J, Demidchik V, Bothwell JHF, et al.** 2003. Reactive oxygen species produced by NADPH oxidase regulate plant cell growth. *Nature* **422**, 442–446.
- Gilroy S, Suzuki N, Miller G, Choi WG, Toyota M, Devireddy AR, Mittler R.** 2014. A tidal wave of signals: calcium and ROS at the forefront of rapid systemic signaling. *Trends in Plant Science* **19**, 623–630.
- Grinstein S, Smith JD, Onizuka R, Cheung RK, Gelfand EW, Benedict S.** 1988. Activation of Na<sup>+</sup>/H<sup>+</sup> exchange and the expression of cellular proto-oncogenes in mitogen- and phorbol ester-treated lymphocyte. *Journal of Biological Chemistry* **263**, 8658–8665.
- Hosy E, Vavasseur A, Mouline K, et al.** 2003. The Arabidopsis outward K<sup>+</sup> channel GORK is involved in regulation of stomatal movements and plant transpiration. *Proceedings of the National Academy of Sciences, USA* **100**, 5549–5554.
- Kinraide TB.** 1998. Three mechanisms for the calcium alleviation of mineral toxicities. *Plant Physiology* **118**, 513–520.
- Knight H, Knight MR.** 2001. Abiotic stress signalling pathways: specificity and cross-talk. *Trends in Plant Science* **6**, 262–267.
- Koyama H, Toda T, Yokota S, Dawair Z, Hara T.** 1995. Effects of aluminium and pH on root growth and cell viability in *Arabidopsis thaliana* strain Landsberg in hydroponic culture. *Plant and Cell Physiology* **36**, 201–205.
- Kumar G, Purty RS, Sharma MP, Singla-Pareek SL, Pareek A.** 2009. Physiological responses among *Brassica* species under salinity stress show strong correlation with transcript abundance for SOS pathway-related genes. *Journal of Plant Physiology* **166**, 507–520.
- Laohavisit A, Shang Z, Rubio L, et al.** 2012. Arabidopsis annexin1 mediates the radical-activated plasma membrane Ca<sup>2+</sup>- and K<sup>+</sup>-permeable conductance in root cells. *The Plant Cell* **24**, 1522–1533.
- Ludwig AA, Romeis T, Jones JD.** 2004. CDPK-mediated signalling pathways: specificity and cross-talk. *Journal of Experimental Botany* **55**, 181–188.
- Maathuis FJ.** 2014. Sodium in plants: perception, signalling, and regulation of sodium fluxes. *Journal of Experimental Botany* **65**, 849–858.
- McAinsh MR, Pittman JK.** 2009. Shaping the calcium signature. *New Phytologist* **181**, 275–294.
- Munns R.** 2002. Comparative physiology of salt and water stress. *Plant, Cell and Environment* **25**, 239–250.
- Munns R, Gilliam M.** 2015. Salinity tolerance of crops—what is the cost? *New Phytologist* **208**, 668–673.
- Munns R, Tester M.** 2008. Mechanisms of salinity tolerance. *Annual Review of Plant Biology* **59**, 651–681.
- Nayidu N, Bollina V, Kagale S.** 2013. Oilseed crop productivity under salt stress. In: Ahmad P, Azouz MM, Prasad MNV, eds. *Ecophysiology and responses of plants under salt stress*. Heidelberg: Springer, 249–265.
- Newman IA.** 2001. Ion transport in plants: measurement of fluxes using ion-selective microelectrodes to characterize transporter function. *Plant, Cell and Environment* **24**, 1–14.
- Niu LJ, Liao WB.** 2016. Hydrogen peroxide signaling in plant development and abiotic responses: crosstalk with nitric oxide and calcium. *Frontiers in Plant Science* **7**, 230.
- Nublat A, Desplans J, Casse F, Berthomieu P.** 2001. Sas1, an Arabidopsis mutant over-accumulating sodium in the shoot, shows deficiency in the control of the root radial transport of sodium. *The Plant Cell* **13**, 125–137.

- Ordoñez NM, Maronedez C, Thomas L, Pasqualini S, Shabala L, Shabala S, Gehring C.** 2014. Cyclic mononucleotides modulate potassium and calcium flux responses to H<sub>2</sub>O<sub>2</sub> in Arabidopsis roots. *FEBS Letters* **588**, 1008–1015.
- Palmgren MG, Nissen P.** 2011. P-Type ATPases. *Annual Review of Biophysics* **40**, 243–266.
- Pandolfi C, Pottosin I, Cuin T, Mancuso S, Shabala S.** 2010. Specificity of polyamine effects on NaCl-induced ion flux kinetics and salt stress amelioration in plants. *Plant and Cell Physiology* **51**, 422–434.
- Purty RS, Kumar G, Singla-Pareek SL, Pareek A.** 2008. Towards salinity tolerance in *Brassica*: an overview. *Physiology and Molecular Biology of Plants* **14**, 39–49.
- Quintero FJ, Martinez-Atienza J, Villalta I, et al.** 2011. Activation of the plasma membrane Na/H antiporter Salt-Overly-Sensitive 1 (SOS1) by phosphorylation of an auto-inhibitory C-terminal domain. *Proceedings of the National Academy of Sciences, USA* **108**, 2611–2616.
- Romani G, Bonza MC, Filippini I, Cerana M, Beggagna N, De Michelis MI.** 2004. Involvement of the plasma membrane Ca<sup>2+</sup>-ATPase in the short-term response of *Arabidopsis thaliana* cultured cells to oligogalacturonides. *Plant Biology* **6**, 192–200.
- Sarkar T, Thankappan R, Kumar A, Mishra GP, Dobarja JR.** 2014. Heterologous expression of the *AtDREB1A* gene in transgenic peanut-conferred tolerance to drought and salinity stresses. *PLoS One* **9**, e110507.
- Schmittgen TD, Livak KJ.** 2008. Analyzing real-time PCR data by the comparative CT method. *Nature Protocols* **3**, 1101–1108.
- Shabala S, Bose J, Fuglsang AT, Pottosin I.** 2016a. On a quest for stress tolerance genes: membrane transporters in sensing and adapting to hostile soils. *Journal of Experimental Botany* **67**, 1015–1031.
- Shabala S, Cuin TA.** 2008. Potassium transport and plant salt tolerance. *Physiologia Plantarum* **133**, 651–669.
- Shabala S, Demidchik V, Shabala L, Cuin TA, Smith SJ, Miller AJ, Davies JM, Newman IA.** 2006. Extracellular Ca<sup>2+</sup> ameliorates NaCl-induced K<sup>+</sup> loss from Arabidopsis root and leaf cells by controlling plasma membrane K<sup>+</sup>-permeable channels. *Plant Physiology* **141**, 1653–1665.
- Shabala S, Newman I.** 2000. Salinity effects on the activity of plasma membrane H<sup>+</sup> and Ca<sup>2+</sup> transporters in bean leaf mesophyll: masking role of the cell wall. *Annals of Botany* **85**, 681–686.
- Shabala S, Newman IA, Morris J.** 1997. Oscillations in H<sup>+</sup> and Ca<sup>2+</sup> ion fluxes around the elongation region of corn roots and effects of external pH. *Plant Physiology* **113**, 111–118.
- Shabala S, Pottosin I.** 2014. Regulation of potassium transport in plants under hostile conditions: implications for abiotic and biotic stress tolerance. *Physiologia Plantarum* **151**, 257–279.
- Shabala S, White RG, Djordjevic MA, Ruan YL, Mathesius U.** 2016b. Root to shoot signalling: integration of diverse molecules, pathways and functions. *Functional Plant Biology* **43**, 87–104.
- Shabala S, Wu H, Bose J.** 2015. Salt stress sensing and early signalling events in plant roots: current knowledge and hypothesis. *Plant Science* **241**, 109–119.
- Shi H, Quintero FJ, Pardo JM, Zhu JK.** 2002. The putative plasma membrane Na<sup>+</sup>/H<sup>+</sup> antiporter SOS1 controls long-distance Na<sup>+</sup> transport in plants. *The Plant Cell* **14**, 465–477.
- Smethurst CF, Rix K, Garnett T, Auricht G, Bayart A, Lane P, Wilson SJ, Shabala S.** 2008. Multiple traits associated with salt tolerance in lucerne: revealing the underlying cellular mechanisms. *Functional Plant Biology* **35**, 640–650.
- Sun J, Chen S, Dai S, et al.** 2009. NaCl-induced alternations of cellular and tissue ion fluxes in roots of salt-resistant and salt-sensitive poplar species. *Plant Physiology* **149**, 1141–1153.
- Sze H, Li X, Palmgren MG.** 1999. Energization of plant cell membranes by H<sup>+</sup>-pumping ATPases: regulation and biosynthesis. *The Plant Cell* **11**, 677–690.
- Véry AA, Nieves-Cordones M, Daly M, Khan I, Fizames C, Sentenac H.** 2014. Molecular biology of K<sup>+</sup> transport across the plant cell membrane: what do we learn from comparison between plant species? *Journal of Plant Physiology* **171**, 748–769.
- Wu H, Zhu M, Shabala L, Zhou M, Shabala S.** 2015. K<sup>+</sup> retention in leaf mesophyll, an overlooked component of salinity tolerance mechanism: a case study for barley. *Journal of Integrative Plant Biology* **57**, 171–185.
- Xie YJ, Xu S, Han B, Wu MZ, Yuan XX, Han Y, Gu Q, Xu DK, Yang Q, Shen WB.** 2011. Evidence of Arabidopsis salt acclimation induced by up-regulation of HY1 and the regulatory role of RbohD-derived reactive oxygen species synthesis. *The Plant Journal* **66**, 280–292.
- Yang Y, Xu S, An L, Chen N.** 2007. NADPH oxidase-dependent hydrogen peroxide production, induced by salinity stress, may be involved in the regulation of total calcium in roots of wheat. *Journal of Plant Physiology* **164**, 1429–1435.
- Zepeda-Jazo I, Velarde-Buendía AM, Enríquez-Figueroa R, Bose J, Shabala S, Muñoz-Murguía J, Pottosin I.** 2011. Polyamines interact with hydroxyl radicals in activating Ca<sup>2+</sup> and K<sup>+</sup> transport across the root epidermal plasma membranes. *Plant Physiology* **157**, 2167–2180.
- Zhu JK.** 2001. Plant salt tolerance. *Trends in Plant Science* **6**, 66–71.
- Zhu JK.** 2003. Regulation of ion homeostasis under salt stress. *Current Opinion in Plant Biology* **6**, 441–445.